Time-Varying Magnetic Field Gradients for Two Dimensional Control of Microswimmers with Cargo

Emma Benjaminson, Department of Mechanical Engineering, Carnegie Mellon University

***Abstract*—Microswimmers are micron-scale robotic devices that can perform tasks in the areas of medicine and manufacturing, such as picking up and delivering cargo to specific locations. However, this task can be difficult to complete because cargo loads can adversely affect the microswimmers' gaits. To compensate, we propose a novel method of controlling microswimmers in two dimensions with a single pair of Helmholtz coils. By opposing the fields of the two coils, we could pull a microswimmer of any shape to a desired location. In this work, we present an initial dynamics model and experimental setup, as well as simulation results and microswimmer rotational motion obtained experimentally. Our results suggest that this control policy could enable visual servoing in two dimensions with one pair of coils and we propose next steps to bring this control policy to fruition. The hope is that we will be able to demonstrate a control policy that could be implemented by existing technology such as magnetic resonance imaging (MRI) machines.**

I. Introduction

Microswimmers are microscale robots that can be actuated externally using magnetic fields. Microswimmers perform a variety of tasks in different fields including drug delivery in medicine [9, 7] and micromanipulation for electronics manufacturing [12]. For many of these applications, microswimmers must be able to carry a cargo load, deliver it to a target site with precision, and then swim to another location to either repeat the process or be retrieved at the end of the procedure. From an implementation perspective, it would be ideal if we could complete all of these steps with a single locomotion strategy.

This problem is interesting because most proposed locomotion strategies to date have been predicated on the assumption that the microswimmer does not change number of links with time. In general, gait design for microswimmers is difficult because they live in a low Reynolds number environment. At low Reynolds numbers, the viscous forces of the fluid dominate the motion of the microswimmer; these viscous forces reverse the motion of reciprocating gaits, resulting in zero net translation. This phenomenon, formulated by Purcell as the Scallop Theorem [13], means that non-reciprocating gaits are essential in order for microswimmers to translate.

The difficulty of designing microswimmer control policies that induce translation as well as pick up and drop off behavior lies in finding a locomotion strategy that is robust to real-time variations in the microswimmer configuration. This is difficult because some researchers rely heavily on their microswimmer design to help them overcome the Scallop Theorem, such as Dreyfus et al [4], and others found that their microswimmers' motion was negatively impacted [8, 7].

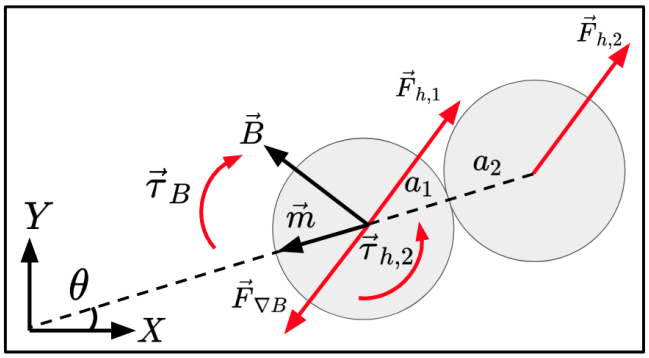

Fig. 1. The single link microswimmer sees a combination of forces and torques acting on it from the fluid as well as the externally applied magnetic field. The left-hand sphere is the magnetic particle of radius a_1 and the right-hand sphere of radius a_2 is the cargo load. $\vec{F}_{h,1}$ and $\vec{F}_{h,2}$ are the hydrodynamic forces applied to sphere 1 and 2, respectively. $\vec{\tau}_{h,2}$ is the torque equivalent of $\vec{F}_{h,2}$ applied to sphere 1. $\vec{\tau}_B$ is the torque applied to sphere 1 by the misalignment between the externally applied magnetic field $\vec{B}$ and the magnetization vector of the sphere, $\vec{m}$. $\vec{F}_{\nabla B}$ is the force applied to the microswimmer by the magnetic field gradient, ∇B.

We propose using the gradient of a magnetic field to pull a microswimmer through a fluid, because applying a simple pulling force is relatively agnostic to the shape of the microswimmer it is manipulating. This approach in itself is not novel, but our method differs from these other approaches because, by changing the shape of the field gradient in real time, we are able to demonstrate complex trajectories in two dimensions with a single pair of Helmholtz coils [3, 2, 7].

To build microswimmers with detachable cargo, we propose using DNA nanotechnology techniques to connect the microswimmer and the cargo. Other researchers have used DNA before, but neither approach demonstrated good control over the length of the DNA structure or the resultant microswimmer structure [10, 4]. We believe this is important not only for maximizing repeatability in the microswimmer's response to a given control input, but also for ensuring that the correct amount of cargo is attached to each microswimmer (an overdose of drug, for example, could have a negative impact on the patient).

The key aspects of our approach are the use of a magnetic field gradient generated from two parallel Helmholtz coils that can have differing magnetic field directions and strengths, which vary over time. We demonstrate that this actuation strategy allows for control in two dimensions. We also show the ability to manufacture microswimmers with DNA nanotechnology.

Statement of Contributions: The first contribution is a novel method of attaching a controlled volume of cargo to a microswimmer in a robust manner. The second is an approach to actuating microswimmers with a magnetic field gradient of whose shape and magnitude varies with time and results in complete control over the microswimmer's position in two dimensions.

II. Related Work

A. Manufacturing Microswimmers with DNA Nanotechnology

As mentioned in the introduction, there are a limited number of examples of building microswimmers with DNA nanotechnology. Of the two works found in our literature review that do use DNA nanotechnology, neither paper demonstrated great control over the decoration of the magnetic particles by the DNA structures, [10, 4]. Maier et al. showed varying numbers of DNA helical structures attached to the magnetic particles, and they also showed varying lengths of DNA structures [10]. These variations suggest that DNA helical tube structures are not good candidates for precisely controlling the physical characteristics of a DNA attachment method (such as length and stiffness), nor are they ideal for ensuring that a fixed amount of cargo is attached to one magnetic particle, since the number of attached DNA structures varied from swimmer to swimmer. In the work done by Dreyfus et al., they were able to control the length of the DNA nanotechnology by using a fixed sequence of nucleic acids in their double-stranded DNA (dsDNA) structure, but they did not show control over the number of dsDNA connections between magnetic particles [4].

B. Managing the Impact of Cargo on Microswimmer Gaits

Some researchers have already demonstrated different methods of carrying cargo with microswimmers, although not all of them have addressed the difficulty of locomoting in both loaded and unloaded configurations. For example, Dreyfus et al. rely on a red blood cell at one end of a chain of superparamagnetic particles to anchor the chain and induce a traveling wave along its length, and in their 2005 paper they do not address whether or not the microswimmer would be able to translate without the red blood cell attached [4]. Further discussion surrounding this work has concluded that although an ideal chain would not have been able to translate without the red blood cell, an applied defect in the connection between the beads would have allowed for net translation through the fluid without a large cargo load [11, 14]. However, adding a defect during construction seems both difficult and counterproductive. Jeon et al. built a rotating microswimmer to carry stem cells but some of their supplementary videos showed that their microswimmers' gait changed from a smooth rotation to a tumbling motion with the introduction of stem cells on board [7]. Overall, Jeon et al.'s results appeared to have a mixed amount of success in different supplementary videos, and the paper itself did not directly address the impact of carrying cargo to the motion of the microswimmer. Lee et al. built a combination cap-and-piston microswimmer which was able to transport cargo on the interior of the cap, but it was not robust enough to be able to secure cargo on the outside of the cap, and there was also no suggestion of how the caps could be retrieved at the end of a procedure, given that only the piston was designed to translate [8].

C. Use of Gradients in Microswimmer Actuation

Magnetic gradients have been considered and applied by various microswimmer researchers to mixed success. Abbott et al. provide a thorough discussion of the relative merits of using gradients compared to other magnetic control methods like rotating fields, and they conclude that gradients are less promising than rotating fields because the gradient falls away as a function of distance to the fourth power (i.e. $\frac{1}{r^4}$) whereas the field falls away as a function of distance to the third power (i.e. $\frac{1}{r^3}$) [2]. Moreover, Abbott et al. show that the forces and velocities induced by a magnetic field gradient also decrease more rapidly than those induced by magnetic fields as the size of the magnetic microswimmer is reduced [2]. But Abbott et al. do not consider changing microswimmer configurations in their discussion, and this paper suggests that the simplest solution to moving a microswimmer whose gait changes significantly with the addition of a cargo load is to pull it with a magnetic field gradient. This approach also makes sense from a practicality standpoint: Nelson et al. point out that current medical tools like magnetic resonance imaging (MRI) machines already use magnetic gradients in their primary mode of operation, so it makes sense to try to leverage this existing capability [11].

III. Theoretical Methods

In this section we will present our mathematical model for the forces and torques applied to a magnetic microswimmer in a magnetic field gradient, and we will show the results of our dynamics simulations.

A. Hydrodynamic Drag at Low Reynolds Number

Since microswimmers inhabit low Reynolds number environments, we must derive equations for the hydrodynamic drag based on some assumptions that are not present when obtaining equations for hydrodynamic drag at the macroscale. Here we present the equation for the hydrodynamic drag on a sphere, as we will model both the single link swimmer and the cargo load as perfect spheres. First, we assume that the fluid is viscous and incompressible; this allows us to consider the flow only in terms of the distance r from the origin and the polar angle θ. We assume that the flow in the x-y plane (as described by the azimuthal angle ϕ) is axisymmetric. Secondly, we assume that the divergence of the fluid flow is zero. Based on these assumptions, we can derive the following equation for hydrodynamic drag from the Navier-Stokes equation [6]:

$$F = -6\pi\mu a U \tag{1}$$

Where μ is the dynamic viscosity of the fluid, a is the radius of the sphere and U is the velocity of the sphere relative to the fluid.

B. Magnetic Field and Gradient Produced by a Pair of Helmholtz Coils

As mentioned in the introduction, we will use a single pair of Helmholtz coils to create our magnetic field gradient. We will outline the derivation of the expressions for the magnetic field generated by a pair of Helmholtz coils below. We begin with an expression for the vector potential field given a current distribution through a loop of wire:

$$\vec{A}_\phi(\rho, z) = \frac{\mu_0 I a}{\pi} \int_0^{\frac{\pi}{2}} \frac{(2sin^2\phi - 1)d\phi}{\sqrt{(a+\rho)^2 + z^2 - 4a\rho sin^2\phi}} \quad (2)$$

We let $k^2 = \frac{4a\rho}{(a+\rho)^2+z^2}$ and use the complete elliptic integrals of the first ($K(k)$) and second ($E(k)$) kind to obtain a closed form solution for $\vec{A}$:

$$\vec{A}_\phi(\rho, \phi) = \frac{mu_0 I}{\pi k}\sqrt{\frac{a}{\rho}}\left[(1 - \frac{1}{2}k^2)K(k) - E(k)\right] \quad (3)$$

Now we must find the expression for the magnetic field, $\vec{B}$. From vector calculus, we know that if a vector field has zero divergence everywhere (which is true for magnetic fields, and is one of Maxwell's equations) then that field is a curl of some other vector field, e.g.:

$$\text{Since } \nabla \cdot \vec{B} = 0, \text{ then } \vec{B} = \nabla \times \vec{A} \quad (4)$$

Therefore we can write the magnetic field in the ρ and z directions as the curl of $\vec{A}$:

$$\vec{B}_\rho(\rho, z) = -\frac{\partial \vec{A}_\phi}{\partial z} \quad (5)$$

$$\vec{B}_z(\rho, z) = \frac{1}{\rho}\frac{\partial}{\partial \rho}(\rho \vec{A}_\phi) \quad (6)$$

And after some manipulation, this leads to the final expressions:

$$\vec{B}_\rho(\rho, z) = \frac{\mu_0 I}{2\pi}\frac{z}{\rho\sqrt{(\rho+a)^2+z^2}}\left[\frac{a^2+\rho^2+z^2}{(a-\rho)^2+z^2}E(k) - K(k)\right] \quad (7)$$

$$\vec{B}_z(\rho, z) = \frac{\mu_0 I}{2\pi}\frac{1}{\sqrt{(\rho+a)^2+z^2}}\left[\frac{a^2-\rho^2-z^2}{(a-\rho)^2+z^2}E(k) + K(k)\right] \quad (8)$$

We can verify this result by comparing the field estimated by Eq 7 and 8 with the analytical solution for the field produced by a pair of Helmholtz coils as measured along the z-axis connecting the two loops. Analytically, we set $\rho = 0$, which means that $k = 0$ and therefore the elliptic integrals are $E(0) = K(0) = \frac{\pi}{2}$. It would appear that this would make $\vec{B}_\rho$ indeterminate, but if we apply L'Hopital's rule then $\vec{B}_\rho = 0$. We are then left with an expression for $\vec{B}_z$:

$$\vec{B}_z(\rho, z) = \frac{\mu_0 I a^2}{2(a^2+z^2)^{\frac{3}{2}}} \quad (9)$$

The comparison of the analytical expression in Eq 9 with the results of the model based on Eq 7 and 8 shows close agreement and the peak is around 8.4 mT which is the estimated maximum magnetic field that the coils can produce according to the manufacturer [1].

Now that we have a valid model of the magnetic field produced by a pair of Helmholtz coils, we were able to model the field produced by a pair of coils whose magnetic fields opposed each other. The results are shown in Fig 2. They show that the field gradient is zero in the exact center and the gradient increases closer to the coils.

C. Dynamics Model

The dynamics model is written with respect to the world frame as shown in Fig 1. We have three state variables, x, y and θ. We will sum the forces acting on sphere 1 of the microswimmer shown in Fig 1 to solve for x and y, and we will sum the torques acting about sphere 1 to solve for θ. We can write these dynamics as shown below:

$$\vec{F}_{\nabla B} + \vec{F}_{h,1} = (m_1 + m_2)\begin{bmatrix}\ddot{x}\\ \ddot{y}\end{bmatrix} \quad (10)$$

$$\vec{\tau}_B + \vec{\tau}_{h,2} = (I_1 + I_2)\ddot{\theta} \quad (11)$$

Where I_1 and I_2 are the moments of inertia of each sphere. Notice that while other models for microswimmer motion assume a quasi-static regime because the low Reynolds number environment implies that the microswimmer has no inertia, here we must assume that the microspheres have inertia because they are going to accelerate in the magnetic field gradient towards the sources of the magnetic field [5].

We can plot the motion of the microswimmer through our magnetic gradient field as the gradients reverse direction. In Fig 2, we can see the motion of the microswimmer through the fluid as the field reverses orientation. As a feasibility test, in the next section we will attempt to recreate this trajectory using our experimental setup.

IV. Experimental Approach

In this section we will outline our experimental setup used to experimentally validate our mathematical model. We will also show the early results of our testing and proposed approach for future work.

A. Setup

We use a pair of Helmholtz coils (3B Scientific GmbH) to generate a magnetic field whose maximum magnitude at 2A is approximately 8.4 mT. The field is monitored using a magnetometer (AlphaLabs Inc.) measuring the field along the z-axis at a rate of 0.25Hz with a precision of $\pm$1G, or 0.1mT.

The microswimmers are constructed using a 2-pot process. In one test tube, polystyrene particles coated in ferromagnetic material with a mean diameter of $10.6\mu m$ and a concentration of 1.5×10^7 beads/mL (Spherotech Inc.) are combined with a single strand of DNA (ssDNA) that is 15 base pairs (7.1nm) long and has a concentration of $1.4\mu M$ (IDT Technologies),

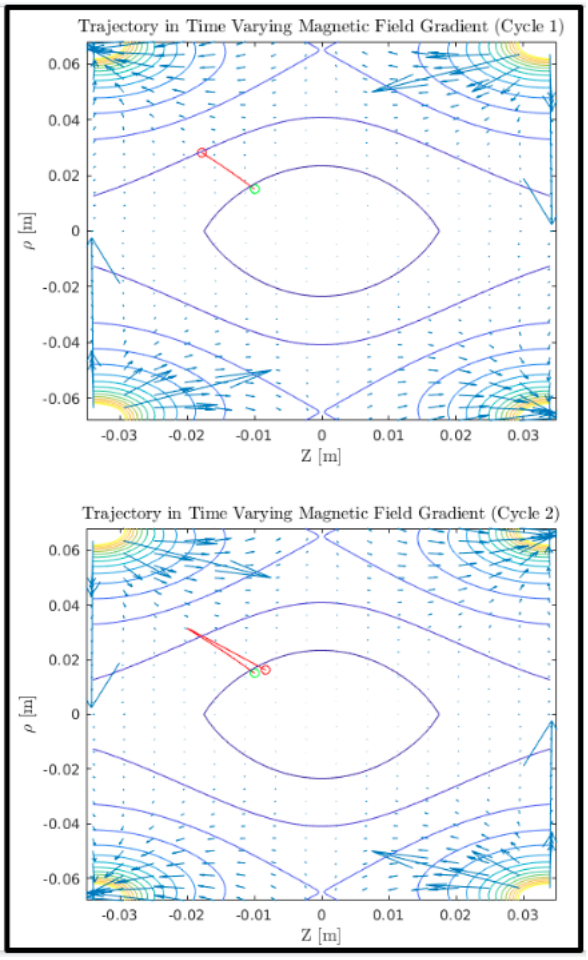

Fig. 2. The top figure shows the first part of the microswimmer's path in the initial magnetic field gradient configuration. The green circle indicates the starting position and the red circle indicates the end point. The bottom figure shows the full trajectory after the magnetic field has reversed direction once.

and then this mixture is diluted with buffer containing Tris-HCL, EDTA and NaCl. In a second tube, the complementary DNA sequence is combined with pure polystyrene particles with a mean diameter of $10.5\mu m$ and a concentration of 7.9×10^6 beads/mL (Spherotech Inc.) and diluted again with buffer. These two pots are incubated separately for 15 minutes at room temperature and then combined and incubated for an additional 15 minutes. A $10\mu L$ sample is then combined with $40\mu L$ of Percoll (Sigma-Aldrich) and flowed into a microfluidic chamber that has been silanized and passivated to reduce surface interactions.

B. Results

In our first test we sent 1.6A to one coil and 0.02A to the other coil in the opposite direction. We measured a magnetic field of about 27G at the point of observation. The direction of flow of the current in each coil was reversed every 25 seconds. We observed that the microswimmer rotated in place to follow the field gradient, but no translation was observed. A kymograph and plot of the applied magnetic field are shown in Fig 4.

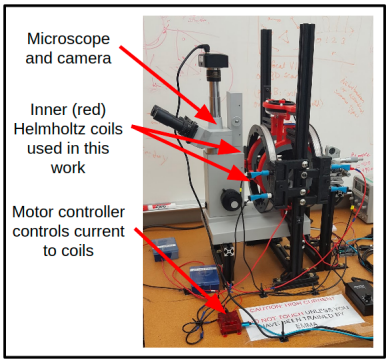

Fig. 3. We use a single pair of Helmholtz coils arranged around an upright microscope to actuate and track the microswimmers constructed using DNA. Note that second pair of Helmholtz coils are shown (black and silver) but are not used in this work.

In our second test, we looked at the effect of creating a shallower magnetic field gradient by sending 1.4A to each coil in opposing directions. We measured a magnetic field of about 5G and reversed the direction of the fields every 25 seconds. We did not observe any response from the microswimmer, indicating that neither the force from the gradient nor the torque from the field direction were strong enough to overcome the resistive forces from the fluid.

These early results indicated that we would need to increase the applied forces and torques from the magnetic field in order to see a response from the microswimmer similar to that seen in our simulations. We magnetized the sample to increase the internal magnetization of the ferromagnetic particulate coating. After magnetization, we noticed that the magnetic particles experienced greater applied torque and they aligned with the magnetic field much more quickly. However, we were unable to find another microswimmer in the sample to test.

V. Conclusion

Our theoretical results suggest that a single pair of Helmholtz coils can indeed induce microswimmer translation in two dimensions. Our early simulations suggest that there is potential for developing a control policy for precise position control. However, our initial testing shows that our experimental setup is able to turn the microswimmers in place, but that the magnetic field gradient is not strong enough to pull the swimmers through the fluid. Our next steps will be to develop a closed loop control policy to move the microswimmer anywhere in the field of observation, and to improve our experimental setup to allow us to pull microswimmers effectively through their fluidic environment.

Acknowledgments

Thank you to my advisors Prof. Taylor and Prof. Travers and to my lab mates in the MMBL and Biorobotics Labs.

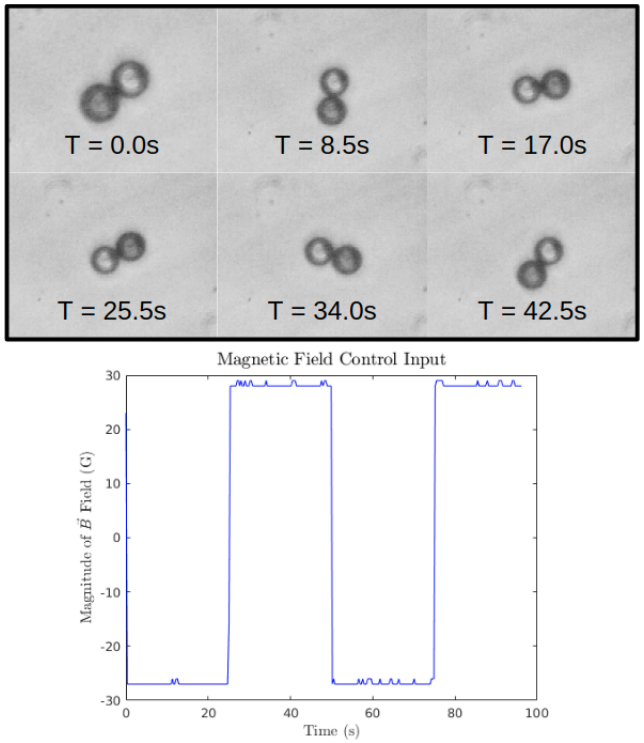

Fig. 4. Top figure is kymograph of rotational motion of single link microswimmer with cargo load attached. Light colored sphere is cargo load, dark sphere is magnetic particle. Microswimmer rotates about cargo load. Bottom figure is magnetic field data as a function of time. As magnetic field changes direction, microswimmer rotates back and forth.

REFERENCES

[1] 3B Scientific ® Physics: Helmholtz Pair of Coils S 1000611. Technical report, 3B Scientific GmbH, 2015. URL www.3bscientific.com.

[2] Jake J Abbott, Kathrin E Peyer, Marco Cosentino Lagomarsino, Li Zhang, Lixin Dong, Ioannis K Kaliakatsos, and Bradley J Nelson. How Should Microrobots Swim? *The International Journal of Robotics Research*, 28(11-12):1434–1447, 2009. doi: 10.1177/0278364909341658. URL https://doi.org/10.1177/0278364909341658.

[3] Christos Bergeles, Bradley E. Kratochvil, and Bradley J. Nelson. Visually Servoing Magnetic Intraocular Microdevices. *IEEE Transactions on Robotics*, 28(4):798–809, 8 2012. ISSN 1552-3098. doi: 10.1109/TRO.2012.2188165. URL http://ieeexplore.ieee.org/document/6168282/.

[4] R Dreyfus, J Baudry, M L Roper, M Fermigier, H A Stone, and J Bibette. Microscopic artificial swimmers. *Nature*, 437(6):2–5, 2005. doi: 10.1038/nature04090.

[5] Jaskaran Grover, Daniel Vedova, Nalini Jain, Matthew Travers, and Howie Choset. Motion Planning, Design Optimization and Fabrication of Ferromagnetic Swimmers. Technical report, Robotics: Science and Systems 2019, Freiburg im Breisgau, 2019. URL http://www.roboticsproceedings.org/rss15/p79.pdf.

[6] E. J. Hinch. Hydrodynamics at low Reynolds numbers: a brief and elementary introduction. 1988. doi: 10.1007/978-94-009-2825-1{_}4.

[7] Sungwoong Jeon, Sangwon Kim, Shinwon Ha, Seungmin Lee, Eunhee Kim, So Yeun Kim, Sun Hwa Park, Jung Ho Jeon, Sung Won Kim, Cheil Moon, Bradley J. Nelson, Jin-young Kim, Seong-Woon Yu, and Hongsoo Choi. Magnetically actuated microrobots as a platform for stem cell transplantation. *Science Robotics*, 4(30):eaav4317, 5 2019. ISSN 2470-9476. doi: 10.1126/scirobotics.aav4317. URL http://robotics.sciencemag.org/lookup/doi/10.1126/scirobotics.aav4317.

[8] Seungmin Lee, Soyeun Kim, Sangwon Kim, Jin-Young Kim, Cheil Moon, Bradley J Nelson, and Hongsoo Choi. A Capsule-Type Microrobot with Pick-and-Drop Motion for Targeted Drug and Cell Delivery. 2018. doi: 10.1002/adhm.201700985. URL https://doi.org/10.1002/adhm.201700985.

[9] Seungmin Lee, Soyeun Kim, Sangwon Kim, Jin-Young Kim, Cheil Moon, Bradley J. Nelson, and Hongsoo Choi. Targeted Drug and Cell Delivery: A Capsule-Type Microrobot with Pick-and-Drop Motion for Targeted Drug and Cell Delivery (Adv. Healthcare Mater. 9/2018). *Advanced Healthcare Materials*, 7(9):1870036, 5 2018. ISSN 21922640. doi: 10.1002/adhm.201870036. URL http://doi.wiley.com/10.1002/adhm.201870036.

[10] Alexander M. Maier, Cornelius Weig, Peter Oswald, Erwin Frey, Peer Fischer, and Tim Liedl. Magnetic Propulsion of Microswimmers with DNA-Based Flagellar Bundles. *Nano Letters*, 16(2):906–910, 2 2016. ISSN 1530-6984. doi: 10.1021/acs.nanolett.5b03716. URL http://pubs.acs.org/doi/10.1021/acs.nanolett.5b03716.

[11] Bradley J. Nelson, Ioannis K. Kaliakatsos, and Jake J. Abbott. Microrobots for Minimally Invasive Medicine. *Annual Review of Biomedical Engineering*, 12(1):55–85, 7 2010. ISSN 1523-9829. doi: 10.1146/annurev-bioeng-010510-103409. URL http://www.ncbi.nlm.nih.gov/pubmed/20415589http://www.annualreviews.org/doi/10.1146/annurev-bioeng-010510-103409.

[12] Chytra Pawashe, Steven Floyd, Eric Diller, and Metin Sitti. Two-Dimensional Autonomous Microparticle Manipulation Strategies for Magnetic Microrobots in Fluidic Environments. *IEEE Transactions on Robotics*, 28(2):467–477, 4 2012. ISSN 1552-3098. doi: 10.1109/TRO.2011.2173835. URL http://ieeexplore.ieee.org/document/6085616/.

[13] E. M. Purcell. Life at low Reynolds number. *American Journal of Physics*, 45(1):3–11, 1 1977. ISSN 0002-9505. doi: 10.1119/1.10903. URL http://aapt.scitation.org/doi/10.1119/1.10903.

[14] M Roper, R Drefus, J Baudry, M Fermigier, J Bibette, and H A Stone. On the dynamics of magnetically driven elastic filaments. *Journal of Fluid Mechanics*, 554:167–190, 2006. doi: 10.1017/S0022112006009049.